NASA/TP-1999-209203



Evaluation of Engineering Properties of Al-Li Alloy X2096-T8A3 Extrusion Products

Y. Flom and M. Viens Goddard Space Flight Center, Greenbelt, Maryland

L. Wang UNISYS, Lanham, Maryland

National Aeronautics and Space Administration

Goddard Space Flight Center Greenbelt, Maryland 20771

The authors would like to thank C. Powers, T. Van Sant, A. Montoya, and C. Taylor for performing measurements of thermal properties, as well as D. Kolos and D. Thomas for their help with metallographic preparation. For more detail regarding their contributions, please contact the authors.

Acknowledgments

Available from:

NASA Center for AeroSpace Information Parkway Center/7121 Standard Drive Hanover, Maryland 21076-1320 Price Code: A17

National Technical Information Service 5285 Port Royal Road Springfield, VA 22161

Price Code: A10

TABLE OF CONTENTS

LIST OF FIGURES	
LIST OF TABLES	
ABSTRACT	1
1. INTRODUCTION	1
2. APPROACH	1
3. AL-LI ALLOY X2096	2
4. TEST RESULTS	4
4.1 Tensile and Comprehensive Properties	4
4.2 Shear and Bearing Properties	5
4.2.1 Shear Test	5
4.2.2 Bearing Test	5
4.3 Elastic Properties	7
4.4 Fracture Properties	8
4.5 Fatigue Properties	ç
4.5.1 Fatigue Crack Growth Rate	9
4.5.2 Bending Fatigue Life	11
4.6 Stress-Corrosion Cracking	12
4.7 Thermal Properties	13
4.7.1 Specific Heat Capacity	13
4.7.2 Thermal Conductivity	
4.7.3 Coefficient of Thermal Expansion	15
4.8 Rivet Test	17
5. DISCUSSION	17
6. CONCLUSIONS	19
LIST OF REFERENCES	21

	· 		
•			
		•	

LIST OF FIGURES

Figure 1.	Photographs of various sections of X2096-TA83 Al-Li alloy extruded beams manufactured at the Reynold's Al casting facility, Richmond, Virginia	2
E. 3	Three dimensional optical micrograph at mid-thickness location in X2096-TA83 extruded beam	
•	(20 sec. Graff-Sargent Reagent, Followed by 15 sec. Keller Etch)	. 3
Figure 3	Low (a) and high (b) magnification optical micrographs of beams cross sections revealing inclusion bands.	
	Linetched	. 3
Figure 4.	Standard pin loaded specimens tested per ASTM E8 and E111. Strain was measured with an averaging	
i iguic 4.	extensioneter with a 2-inch gauge length	.4
Ciaura 5	Stress-strain curves for the "dog-bone" type specimens machined in L direction from the X2096-T8A3 Al-Li alloy	
Figure 5.	extruded beams	5
Ciarra 6	Double slotted single shear test specimens used to measure shear strength of Al-Li extruded beams. A complete description	
Figure 6.	of these tests can be found in Ref. 2	5
Cia 7	Load vs. crosshead displacement curve for one of the shear test specimens	6
rigure /.	Load vs. crossnead displacement curves for the bearing test. There is no noticeable difference in the behavior between	
rigure 8.	Lot 10 (view A) and Lot 9 (view B) specimens	8
E: 0	One of the M(T) center crack specimen used for the R-curve and K _c tests	. 9
Figure 9.	R curves of the tested Al-Li X2096-T8A3 extruded beam specimens. Specimen ID contains the Lot, orientation	
Figure 10.	and specimen number	10
 11	Fracture surfaces of the test specimens showing V-slant morphology. Arrows point to the fatigue precracked	
Figure 11.	ends of the initial crack length 2a ₀	10
r: 10	ends of the initial crack length za ₀	
Figure 12.	A typical crack length vs. cycle number plot obtained by compliance method and optical measurements	I 1
	measurements	
Figure 13.	Al-Li alloy. Specimens ID indicates the lot, orientation, and the specimen number	11
	Al-Li alloy. Specimens ID indicates the lot, orientation, and the specimen number.	12
Figure 14.	A cantilever beam specimen used for bending fatigue test	
Figure 15.	Fatigue life curves for the X2096-TA83 Al-Li alloy extruded beams measured in L and LT orientation.	13
	Specimen nomenclature L-T and T-L is the same as defined in section 4.4	14
Figure 16.	Specific heat capacity for the Reynolds X2096-T8A3 Al-Li alloy extruded beams	15
Figure 17.	Thermal diffusivity as a function of temperature for the Reynolds X2096-T8A3 Al-Li alloy extruded beams	15
Figure 18.	Thermal conductivity as a function of temperature for the Reynolds X2096-T8A3 Al-Li alloy extruded beams	.10
Figure 19.	Linear expansion of the Reynolds X2096-T8A3 Al-Li alloy extruded beam specimens testing in L and LT	17
	directions	17
Figure 20	Coefficient of thermal expansion vs. temperature for the Reynolds X2096-T8A3 Al-Li alloy specimens	1 /
Figure 21	Longitudinal cross section of the riveted joint. White arrows point to the surfaces of the Al-Li alloy that were	1 2
	inspected for cracks	.10 21
Figure 22	Fracture surface of the broken strip machined from the X2096-T8A3 extrusion. Note severe delamination	, 21
Figure 23	Behavior of the X2096-T8A3 strip machined from the extruded beam in transverse (a) and longitudinal (b)	21
	bending. Note delamination in longitudinal bend	41
	LIST OF TABLES	
Table 1.	Minimum Properties Specified in Purchase Request	l
Table 2.	Property Test Program	I
Table 3	Composition of X2096 Al-Li alloy beams	2
Table 4.	Tensile and Compressive Properties of RMC Al-Li alloy X2096-T8A3 Extruded Beams Tested at RMC	4
Table 5.	Results of tensile test of X2096-T8A3 Al-Li alloy extrusion beam specimens in L direction.	
	The tests were performed at Goddard	5
Table 6.	Shear Strength of X2096-T8A3 Al-Li Extruded Beams	t
Table 7.	Bearing Properties of X2096-T8A3 Al-Li alloy	7
	• •	

LIST OF TABLES (continued)

Table 8.	Results of acoustic resonance testing of the Reynolds X2096-T8A3 Al-Li alloy specimens machined	
	from extruded beams	9
Table 9.	K _c values for X2096-T8A3	9
	. Stress calculations using four different methods	
	. Coefficient of Thermal Expansion vs. Temperature for X2096 Al-Li alloy	
Table 12	. Statistical Analysis of Results.	19

ABSTRACT

Mechanical, thermal, fatigue and stress corrosion properties were determined for the two lots of Al-Li X2096-T8A3 extruded beams. Based on the test results, the beams were accepted as the construction material for fabrication of the Hubble Space Telescope new Solar Array Support Structure.

1.0 INTRODUCTION

Potential property advantages of Al-Li alloys present an attractive alternative to the conventional 7075 alloy in structural design for aerospace applications. An increase in weight savings and performance enticed the Hubble Space Telescope (HST) project team to consider these alloys for construction of the support frame of the new Solar Array (SA3) Panels that will replace the existing array during the next servicing mission.

The HST project team selected the Reynolds Metal Company (RMC) X2096 alloy as their material of choice for its low density, high elastic modulus, high strength, and toughness. Since the commercial utilization of Al-Li alloys is still limited, X2096 alloy is not produced on regular basis and is not part of MIL HDBK 5. Consequently, this alloy had to be treated as a new product and its properties had to be tested in order to qualify this material for the space flight application.

This memorandum provides a detailed account of testing performed by the Materials Engineering Branch (MEB) to verify the properties of the RMC X2096 Al-Li alloy. It also presents test results obtained by the Reynolds Metal Company and forwarded to the Goddard Space Flight Center (GSFC).

2.0 APPROACH

The minimum required properties of X2096 Al-Li alloy specified by the HST project in the Purchase Request issued to RMC are presented in Table 1. The material was produced and extruded by RMC and delivered to Goddard in form of the rectangular and round tubes (beams).

The test program was divided between the GSFC MEB and RMC as shown in Table 2. The rationale of doing part of the tests by RMC was to save time by performing the tests in parallel. In addition, RMC was to perform some basic mechanical testing *anyway* as part of their internal product release requirements.

The specimens tested by MEB were machined (see Attachment for geometry and dimensional details) from the extruded rectangular beams representing both lots. Sampling and testing of the round tubes were performed by RMC. However, due to the fact that the number of extruded beams was limited and most of the material was required for manufacturing of the support structure, only one lot was tested by RMC.

In addition to the tests listed in Table 2, MEB performed several tensile tests for verification purposes only. The information derived from these tests was used to baseline the properties of the extruded beams.

Table 1. Minimum Properties Specified in Purchase Request

Orientation	Ultimate Tensile	Tensile Yield	Elongation,	Compressive	Stress Corrosion
	stress,	Stress,	%	Yield Stress,	Test Stress Level,
	ksi	ksi		ksi	% of Tensile Yield
L	76	73	7	69	
L-T	75	70	7		75

Table 2. Property Test Program

Test Site		Test Type								
Goddard MEB	Bearing	Shear	Fracture toughness	Fatigue	Thermal	Rivet				
RMC	Tensile	Compression	Stress Corrosion		<u> </u>					

3.0 AL-LI ALLOY X2096

In response to PR from GSFC, RMC produced two X2096 Al-Li alloy ingots of 9,000 and 10,000 lbs. Each ingot was cut into 30-40 round billets of approximately 10 inches in diameter and 10 inches in length. A through hole of 5-inch diameter was drilled in each billet. This was followed by extrusion of the billets into rectangular and round tubes (beams). Thus, two lots of beams were produced. All beams were heat treated to the RMC proprietary T8A3 temper. The lot that came from the 9,000 lbs ingot was identified as Lot 9 and, likewise, the beams from the 10,000 lbs ingot were identified as Lot 10. This lot nomenclature was used for

tracking and quality assurance purposes by GSFC and RMC and, consequently, will be used as such throughout this report.

The rectangular beams received by MEB for testing are shown in Fig. 1.

Wall thickness measurements showed variation in thickness from 0.080 to 0.100 inches. Samples from each lot were analyzed for chemical composition. The results of Inductively Coupled Plasma Optical Emission Spectroscopy analysis are presented in Table 3.



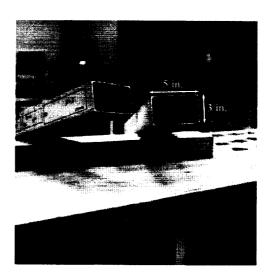


Figure 1. Photographs of various sections of X2096-TA83 Al-Li alloy extruded beams manufactured at the Reynold's Al casting facility, Richmond, Virginia.

Table 3 Composition of X2096 Al-Li alloy beams

	Nominal composition of X2096 alloy *	Lot 9 (wt%)	Lot 10 (wt%)
	(wt%)	(W(70)	(W17C)
Copper	2.3 – 3.0	3.1	2.9
Lithium	1.3 – 1.9	1.7	1.6
Magnesium	0.25 - 0.80	0.31	0.29
Silver	0.25 - 0.60	0.2	0.2
Zirconium	0.04 - 0.16	0.14	0.13
Manganese	0.25 max.	0.03	0.01
Zinc	0.25 max.	0.02	0.02
Iron	0.15 max.	0.05	0.06
Silicon	0.12 max.	0.04	0.04
Titanium	0.10 max.	0.02	0.02
Aluminum	Remainder	Remainder	Remainder

^{* -}composition registered with the Aluminum Association.

As one can see, silver content in the extruded beams was somewhat below the expected range.

Samples from each lot were also metallographically cross sectioned and polished to reveal their grain structure. Three-dimensional optical micrograph of the cross section of the extruded beam wall is shown in Fig.2.

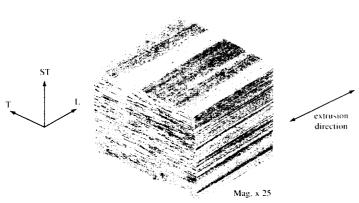


Figure 2. Three dimensional optical micrograph at mid-thickness location in X2096-TA83 extruded beam (20 sec. Graff-Sargent Reagent, Followed by 15 sec. Keller Etch).

This micrograph represents typical microstructures obtained for each lot. In all cases, the alloy X2096 microstructure shows mostly unrecrystallized pancake-shape grains elongated in direction of extrusion. An unusual feature was observed on unetched cross sections of the extruded beams. Bands of inclusions were present below the surfaces of the beam walls, as shown in Figure 3.

An attempt to analyze these inclusions was made using Auger microscopy. Only aluminum and oxygen were detected in the inclusion material. In addition, a tape lifting technique was utilized on the fracture surfaces of the mechanically tested samples later on in the program. Again, SEM spectroscopy did not reveal the presence of any elements other than aluminum. It is believed, therefore, that the inclusions consist of aluminum oxide trapped into the beam material during the manufacturing process. It is not clear, however, why these inclusions were arranged into subsurface bands. No satisfactory explanation from RMC was provided on the nature of these inclusion bands.

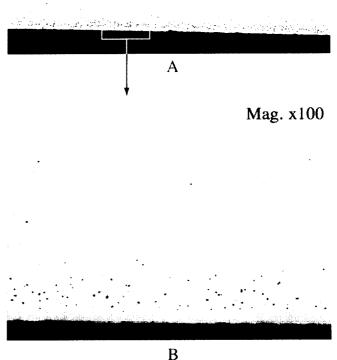


Figure 3. Low (a) and high (b) magnification optical micrographs of beams cross sections revealing inclusion bands. Unetched.

4.0 TEST RESULTS

4.1 Tensile and Compressive Properties.

RMC measured tensile and compressive properties of the Lot 9 extruded beams and forwarded their results to GSFC to be included in this report. Due to the beam size limitation, subsize tensile specimens were used for tension test. The geometry of the tensile or compression test specimens or the tests details were not provided to Goddard (see Ref. 1). The test results received from the RMC are summarized in Table 4.

As one can see, these properties exceed the requirements of the PR listed in Table 1.

Prior to and independent from the RMC tensile test effort, MEB also performed a limited number of tensile tests in order to better understand the properties of the newly received extruded beams. Full size "dog bone" type specimens were machined from the beams representing both Lots 9 and 10 (see Figure 4). All specimens were oriented in L direction.

The test results are presented in Table 5. Modulus of elasticity E was calculated using the average of three loading cycles and taken as the slope of the stress strain data between 0.05% and 0.25% strain, per ASTM E-111.

The average value of E was found to be 10.99 Msi, which is in agreement with the elastic properties determined using the acoustic resonance technique

A full range stress-strain behavior of the tensile test specimens is shown in Figure 5.

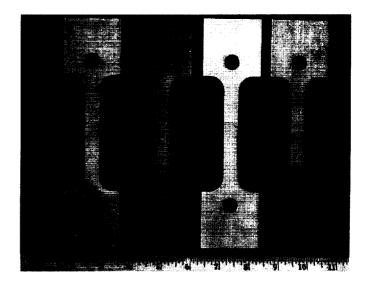


Figure 4. Standard pin loaded specimens tested per ASTM E8 and E111. Strain was measured with an averaging extensometer with a 2-inch gauge length.

Table 4. Tensile and Compressive Properties of RMC Al-Li alloy X2096-T8A3 Extruded Beams Tested at RMC

DIRECTION		COMPRESSION TEST		
DIRECTION	Tensile Yield	Ultimate Tensile	Elongation	Compressive Yield
	Stress (ksi)	Stress (ksi)	%	Stress (ksi)
L	71.5	79.5	9.0	79.4
L	75.8	80.9	9.0	77.1
L	74.9	80.2	9.0	
L-T	72.7	77.2	10.0	78.8
L-T	70.4	76.5	8.0	76.1
45 deg.	60.6	67.1	12.0	69.2
45 deg.	61.0	67.5	12.0	71.0

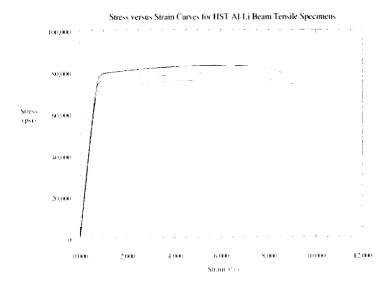


Figure 5. Stress-strain curves for the "dog-bone" type specimens machined in L direction from the X2096-T8A3 Al-Li alloy extruded beams.

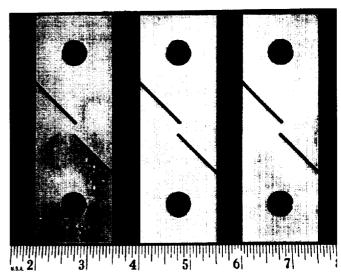


Figure 6. Double slotted single shear test specimens used to measure shear strength of Al-Li extruded beams. A complete description of these tests can be found in Ref. 2.

4.2 Shear and Bearing Properties

4.2.1 Shear Test

The shear strength was measured in L and L-T directions on Lot 9 and 10 beam specimens. Since no ASTM standard is available for shear test of thin plate/sheet material, the double slotted single shear tests were selected (see Fig. 6) The specimens were EDM machined from the beam sides. Due to beam wall thickness variation, thickness of the test specimens measured from 0.082 to 0.100 inches. A typical shear loading curve is shown in Fig. 7

An Instron 1125 universal testing machine was used to load the specimens to failure at a crosshead speed of 0.05 inches per minute.

The results of the double slotted single shear tests are given in Table 6.

Table 5. Results of tensile test of X2096-T8A3 Al-Li alloy extrusion beam specimens in L direction.

The tests were performed at Goddard

ID	Thickness	Width	Yield	Ultimate	Young's*	Elongation
(lot/spec.#)	(in)	(in)	Strength	Strength	Modulus	at Failure
			(ksi)	(ksi)	(Msi)	(%)
9-1	0.0950	0.5015	78.30	82.66	10.96	8.8
9-2	0.0940	0.5015	78.72	82.86	11.11	8.1
10-1	0.0996	0.5015	71.06	76.00	10.88	9.1
10-2	0.0974	0.4995	74.95	79.14	10.99	9.6

^{*} Taken as chord between 0.05 and 0.25% strain

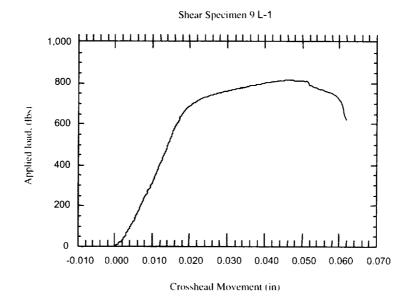


Figure 7. Load vs. crosshead displacement curve for one of the shear test specimens.

An Instron 1125 universal testing machine was used to load the specimens to failure at a crosshead speed of 0.05 inches per minute.

L specimens. Specimens representing Lot 9 seem to be somewhat stronger than the specimens from Lot 10.

The results of the double slotted single shear tests are given n Table 6.

4.2.2 Bearing Test

The average shear strength was found to be 47.50 ± 0.77 ksi. The L-T specimens tend to be slightly stronger than the

The bearing properties of the Al-Li alloy were measured in accordance with ASTM E 238 for edge distance-to-diameter ratios (e/D) of 1.5 and 2. Specimens were loaded

Table 6. Shear Strength of X2096-T8A3 Al-Li Extruded Beams

Specimen ID	Thickness	Ligament	Maximum	Ultimate Shear
(lot, orientation, spec.#)	(in)	Length	Load	Stress F _{su}
		(in)	(lbs)	(ksi)
9 L-1	0.0925	0.1854	817.7	47.68
9 L-2	0.0960	0.1865	852.1	47.59
9 L-3	0.0925	0.1865	822.0	47.65
9 LT-1	0.0865	0.1874	793.6	48.96
9 LT-2	0.0830	0.1866	745.0	48.10
9 LT-3	0.0825	0.1865	737.7	47.95
10 L-1	0.0990	0.1867	846.7	45.81
10 L-2	0.0930	0.1866	824.7	47.52
10 L-3	0.0930	0.1865	812.3	46.83
10 L-4	0.0935	0.1858	811.3	46.70
10 LT-1	0.0875	0.1842	758.7	47.07
10 LT-2	0.0900	0.1854	795.2	47.66
10 LT-3	0.0890	0.1863	796.2	48.02

to failure in Instron 1125 universal test machine at crosshead speed of 0.05 inches per minute. The results of bearing test are presented in Table 7.

Specimens 10-L-5 through 8 in Table 7 have somewhat lower values of the bearing ultimate stress. The rest of the specimens exhibited quite consistent behavior and showed no difference in bearing properties between Lot 9 and Lot 10. Also, specimen orientation did not seem to affect their bearing properties.

4.3 Elastic Properties

The elastic properties of the Reynolds X2096-T8A3 Al-Li alloy extruded beams were measured in L and L-T directions using acoustic resonance technique in accordance with ASTM standard C 1259-94. More detailed description of this technique can be found in Reference 3.

The test results are presented in Table 8.

Table 7. Bearing Properties of X2096-T8A3 Al-Li alloy

Specimen ID	Thickness	Pin	e/D	Yield	Max	Bearing	Bearing
(lot, orientation,	(in)	Diameter		Load	Load	Yield Stress	Ultimate Stress
spec.#)		(in)		(lbs)	(lbs)	F _{bry} (ksi)	F _{bru} (ksi)
9 L-1	0.097	0.249	2	2867	3635	118.2	149.9
9 L-2*	0.097	0.249	2		3582		148.8
9 L-3	0.096	0.249	2	2830	3605	118.1	150.4
9 L-5	0.097	0.248	1.5	2167	2767	90.5	115.5
9 L-6	0.097	0.249	1.5	2378	2740	98.7	113.7
9 L-7	0.097	0.249	1.5	2394	2774	99.3	115.0
9 LT-1	0.089	0.249	2	2662	3335	120.0	150.3
9 LT-2	0.090	0.249	2	2569	3366	114.4	149.9
9 LT-3*	0.090	0.249	2		3368		150.6
9 LT-4	0.089	0.250	1.5	2194	2547	98.5	114.3
9 LT-5	0.089	0.249	1.5	2106	2559	95.0	115.4
9 LT-6	0.089	0.249	1.5	2154	2515	96.8	113.0
10 L-1	0.094	0.247	2	2774	3431	119.5	147.8
10 L-2	0.092	0.249	2	2588	3304	113.0	144.3
10 L-3	0.091	0.245	2	2643	3246	118.0	145.0
10 L-4	0.091	0.248	2	2681	3389	118.3	149.6
10 L-5	0.094	0.249	1.5	2202	2601	93.9	110.9
10 L-6	0.094	0.249	1.5	2074	2522	88.6	107.8
10 L-7	0.100	0.248	1.5	2266	2658	91.8	107.7
10 L-8	0.092	0.248	1.5	2170	2537	95.5	111.6
10 LT-1	0.087	0.249	2	2569	3182	118.7	147.1
10 LT-2	0.085	0.249	2	2364	3144	111.4	148.2
10 LT-1	0.091	0.250	2	2715	3372	118.8	147.5
10 LT-2	0.091	0.247	2	2755	3430	123.2	153.4
10 LT-3	0.087	0.249	1.5	2061	2394	95.5	111.0
10 LT-4	0.088	0.249	1.5	2089	2460	95.8	112.8
10 LT-3	0.081	0.248	1.5	1928	2301	96.6	115.3
10 LT-4	0.090	0.249	1.5	2219	2653	99.1	118.5

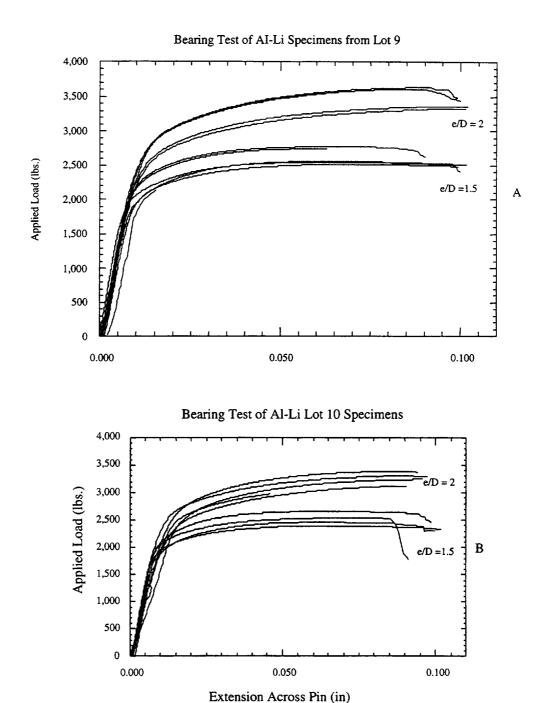


Figure 8. Load vs. displacement curves for the bearing test. There is no noticeable difference in the behavior between Lot 10 (view A) and Lot 9 (view B) specimens.

Table 8. Results of acoustic resonance testing of the Reynolds X2096-T8A3 Al-Li alloy specimens machined from extruded beams

ID	Length	Thickness	Width	Dens.	POISSON	R[FLEX]	R[LONG]				
	(in)	(in)	(in)	(g/cm3)	Ratio	kHz	kHz	kHz		Modulus	
									Msi	Msi	Msi
10-L-1	4.002	0.095	1.501	2.59	0.43	1.281	26.66	1.972	10.81	11.19	3.79
10-L-2	4.002	0.091	1.502	2.61	0.40	1.239	26.64	1.926	10.98	11.25	3.92
10-LT-1	4.000	0.090	1.500	2.64	0.40	1.219	26.55	1.895	10.97	11.30	3.91
10-LT-2	4.000	0.090	1.500	2.64	0.40	1.220	26.55	1.898	10.98	11.29	3.92
10-LT-3	4.001	0.091	1.501	2.60	0.40	1.219	26.55	1.894	10.57	11.15	3.77
10-LT-4	4.000	0.090	1.502	2.63	0.40	1.217	26.55	1.891	10.84	11.25	3.87
9-L-1	4.002	0.098	1.502	2.60	0.42	1.338	26.68	2.060	11.00	11.26	3.87
9-L-2	4.002	0.095	1.502	2.60	0.42	1.288	26.68	1.985	10.96	11.26	3.85
9-L-3	4.002	0.099	1.502	2.60	0.42	1.341	26.68	2.065	10.96	11.25	3.85
9-LT-1	4.001	0.085	1.502	2.60	0.41	1.140	26.67	1.768	10.68	11.22	3.78
9-LT-2	4.002	0.085	1.505	2.59	0.40	1.138	26.67	1.767	10.68	11.19	3.80
9-LT-3	4.002	0.084	1.502	2.62	0.43	1.143	26.68	1.765	11.14	11.34	3.91

The average in-plane elastic modulus or Modulus of Elastic E was found to be 11.25±0.05 Msi. Scatter in density and elastic properties measurements is most likely due to non-uniform thickness and flatness of the extruded beams.

4.4 Fracture Properties.

Crack extension resistance curve (R-Curve) and planestress fracture toughness K_c tests were performed on the specimens machined from the Lots 9 and 10 of the Reynolds X2096-T8A3 Al-Li alloy extruded beams. Due to the beam size limitations, the specimens were machined only in L direction. The tests were conducted in accordance with ASTM E-561 and B-646 standards as applied for sheet products. The center crack plate configuration (M(T)) of the test specimens is shown in Figure 9. The tests were per

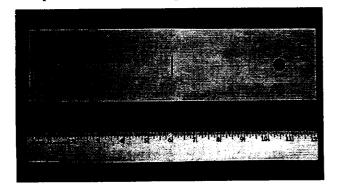


Figure 9. One of the M(T) center crack specimen used for the R-curve and K_c tests.

formed on computer controlled Instron Model 1350 dynamic testing system equipped with the Instron Fast-TrackTM software.

The thickness of the test specimens ranged from 0.082 to 0.095 inch due to variations in the beam wall thickness. The center notch was EDM machined as per the specimen drawing in the Attachment. Each specimen was precrackedin axial tensile-tensile fatigue to the nominal initial crack length (2a₂) of 1 inch.

A total of five specimens were tested. Table 9 lists the K_c values obtained. Figure 10 shows R-curve, a plot of crack-extension resistance as a function of slow-stable crack extension, obtained for each specimen. The effective crack length was determined by using the compliance method. The effective crack growth was primarily due to plastic zone correction. The fracture surfaces of the test specimens show mostly V-slant morphology (see Figure 11), which indicates that the specimens were tested in plane-stress condition.

Table 9. K_c values for X2096-T8A3

Sample ID	Kc, ksi • in ^{0.5}
9-L1	41.3
9-L2	46.6
9-L3	50.6
10-L1	47.2
10-L2	43.3

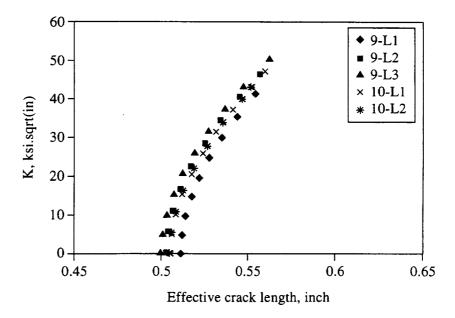


Figure 10. R curves of the tested Al-Li X2096-T8A3 extruded beam specimens. Specimen ID contains the Lot, orientation and specimen number.

4.5 Fatigue Properties

Fatigue crack growth rate and the endurance limit measurements were performed using tension-tension and bending fatigue test methods as described below.

4.5.1 Fatigue Crack Growth Rate

The center crack plate M(T) configuration test specimens were machined from the extruded beams in L (longitudinal) and LT (long transverse) directions. Two specimen widths were used, 1.5- and 3.0-inch, with the nominal precrack length (2a) of 0.27- and 1-inch respectively. The specimen's thickness varied from 0.075 to 0.095 inch.The complete specimen geometry is given in the drawings in the Appendix. Due to the extruded beam size, the 3 x 12 inch specimens could only be machined in L direction.

The tests were conducted in accordance with the ASTM E-647 standard. The constant load method was used and the stress ratio R was maintained at 0.1 for the entire test. Fatigue crack lengths was measured using the compliance method. In this method, the compliance data were used to fit into the initial and final crack lengths to obtain the crack length data for every incremental crack growth by adjusting the apparent modulus and the Crack Opening Displacement. The data were then compared with those using optical

measurement for each specimen. The correlation between these two methods was found to be very good, as can be seen in Figure 12 showing a typical plot of crack length vs. number of cycles.

The next figure shows a plot of the fatigue crack growth rate (da/dN) vs. stress intensity factor amplitude ΔK . Crack growth rate for the 7075-T7351 alloy is also shown on the same plot for comparison.

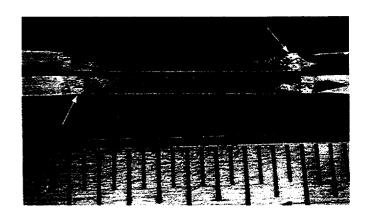


Figure 11. Fracture surfaces of the test specimens showing V-slant morphology. Arrows point to the fatigue precracked ends of the initial crack length 2a,.

Specimen 9L2, 1.5 inch wide

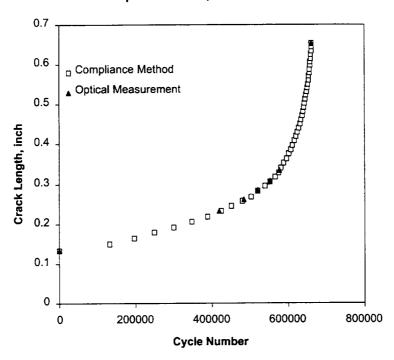


Figure 12. A typical crack length vs. cycle number plot obtained by compliance method and optical measurements.

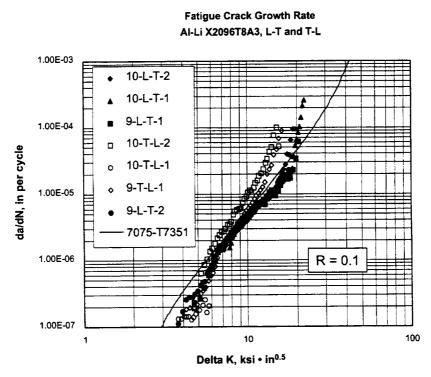


Figure 13. Shows a plot of da/dN vs. ΔK for the test specimens machined from the extruded beams of X2096-T8A3 Al-Li alloy. Specimens ID indicates the lot, orientation, and the specimen number.

The nomenclature L-T and T-L is more convenient in this case since it better identifies the loading direction (the first letter) and the direction of crack propagation (the second letter).

4.5.2 Bending Fatigue Life

The bending fatigue endurance limit of the extruded beams was measured in L and LT directions per ASTM B 593 using subsized cantilever beam specimen geometry. The geometry allows for a constant stress to be maintained along the entire gauge length of the test specimen (see Figure 14).

The specimens were tested on Satec SF-2U constant force fatigue machine. Although reliable and quite simple in operation, this machine does not allow for an active and precise control of the applied load. The load can only be changed by varying the moment arm on a weight that spins beneath the loading yoke. This type of loading is difficult to calibrate. Therefore, a strain gauge was employed to measure the strains and calculate the stresses on the test specimens.

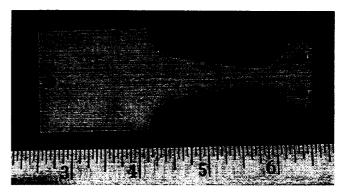


Figure 14. A cantilever beam specimen used for bending fatigue test.

Table 10. Stress calculations using four different methods

Specimen ID	Cycles to failure	Maximum s	tress values obtai	Average Stress	Standard Deviation		
	·	Applied Load, $\sigma = 18P/h^2$	Theoretical Slope, σ = Eyh/5.0625	Measured Slope, σ = Eym	Measured Strain, σ = Ee		
10-LT-1	46000	36.36	32.68	29.83	31.90	32.69	2.73
10-LT-2	73000		34.04	26.78	31.24	30.69	3.66
10-LT-3	115000	28.74	24.27	20.89	22.66	24.14	3.36
9-LT-1	265000	24.82	23.21	17.66	18.48	21.04	3.51
9-LT-2	735000	21.11	19.09	17.31	17.05	18.64	1.88
9-LT-3	1615000	18.29	17.04	13.98	14.19	15.88	2.13
9-LT-4	10933000	15.56	15.18	12.25	12.76	13.93	1.67
9-L-1	119000		32.48	28.65	31.24	30.79	1.95
9-L-2	153000		34.99	27.74	29.81	30.85	3.73
10-L-1	199000	30.43	28.81	26.44	26.62	28.07	1.90
10-L-2	256000	29.14	25.30	20.67	23.43	24.63	3.55
10-L-3	439000	22.96	24.03	20.17	21.34	22.12	1.71
9-L-3	444000	25.52	24.79	19.96	21.34	22.90	2.68
10-L-4	545000	27.22	28.46	22.43	24.86	25.74	2.66
10-L-5	962000		17.87	14.82	15.62	16.10	1.58
9-L-4	14740000	18.33	15.20	12.23	11.66	14.36	3.07
10-L-6	24896000	15.61	15.03	12.95	13.31	14.22	1.30
10-L-7	25379000	18.73	17.58	14.91	15.62	16.71	1.76

Note: P – applied load, y – observed deflection, m – calibrated slope, e- observed strain, h– specimen thickness, E – elastic modulus taken to be 11 Msi.

There were a total of four methods employed to calculate stresses in each test specimen. These stresses are presented in Table 10. The average and standard deviation values were calculated using the maximum stresses from the various calculation methods. This assumes that the failure was initiated on the surface with the higher stress.

The fatigue life is represented by the stress vs. cycles to failure plot as shown in Fig. 15.

The error bars represent the difference observed in the calculation of the stress values. The lower bound to the curves could be used to generate a conservative fatigue life prediction. Regardless of the problems associated with the stress calculations, the LT specimens clearly have a slightly lower fatigue life. This observation is consistent with the da/dN results described in section 4.4. As one can see in Figure 13, the T-L specimens displayed higher crack growth rate than the L-T ones.

4.6 Stress-Corrosion Cracking

Stress-corrosion testing was performed by RMC at their Corporate Research and Development facility in Chester, Virginia.

Due to the insufficient amount of the beam material available, only the Lot 9 specimens were tested. The test was conducted per ASTM G39-90 procedure using double bent beam setup. The results of the test are given below.

Specimen ID	Stress (ksi)	Test Duration (days)	No. Specimens Tested	Failures	Time to Failure
0220-09	50	30	4	0	

Al-Li Bending Data

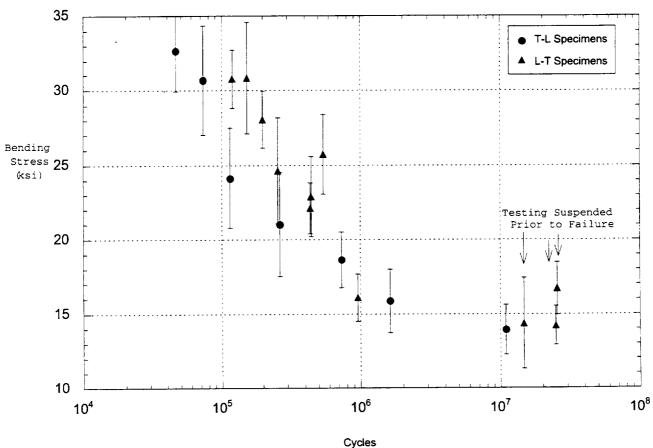


Figure 15. Fatigue life curves for the X2096-TA83 Al-Li alloy extruded beams measured in L and LT orientation.

Specimen nomenclature L-T and T-L is the same as defined in section 4.4.

Specimens were machined from the X2096-T8A3 Al-Li extruded beams. Their thickness was 0.090 and the length was 4.25 inch. They were all oriented in LT direction. The test environment was 3.5% NaCl alternate immersion, as per ASTM Standard G44. Moderate pitting was observed at the end of the test.

This is the extent of information supplied by RMC (see Reference 1).

4.7 Thermal Properties

4.7.1 Specific Heat Capacity

Six specimens of the Reynolds X2096-T8A3 Al-Li alloy were used to measure specific heat capacity C_p between – 100°C and 100°C. These specimens represented Lot 9 and 10

The specimens were tested using differential scanning calorimetry (DSC) according to ASTM E-1269. The specimens were heated at 20°C/minute in a helium atmosphere. Each specimen was tested five times and the average results calculated for each temperature.

The plot in Figure 16 details the specific heat values between 50°C and 100°C. Below 50°C the DSC instrument behaved erratically, and the data obtained below 50°C could not be considered valid. Consequently, these data are not reported in this memorandum.

4.7.2 Thermal Conductivity

Thermal conductivity was calculated from thermal diffusivity (γ) , specific heat (C_p) , and density (d) using the following equation:

$$q = \gamma C_0 d$$
 (see Ref. 4).

Thermal diffusivity was measured using the Angstrom's temperature wave method. A peltier junction was used to generate a periodic heat wave along a specimen. Two thermocouples were used to measure the decay in amplitude and phase shift of the heat wave as it traveled along the specimen. These two parameters were used to calculate thermal diffusivity (see Ref. 4 for a detailed discussion).

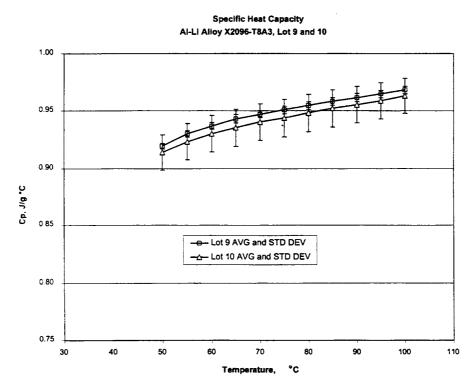


Figure 16. Specific heat capacity for the Reynolds X2096-T8A3 Al-Li alloy extruded beams.

Thermal Diffusivity of Al-Li Extruded Beams

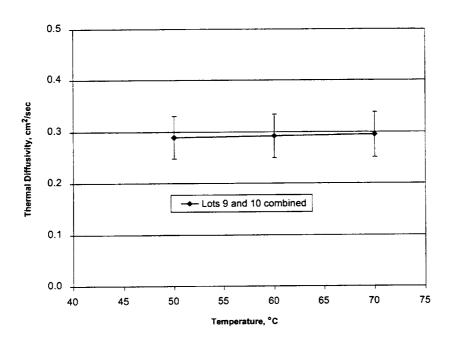


Figure 17. Thermal diffusivity as a function of temperature for the Reynolds X2096-T8A3 Al-Li alloy extruded beams.

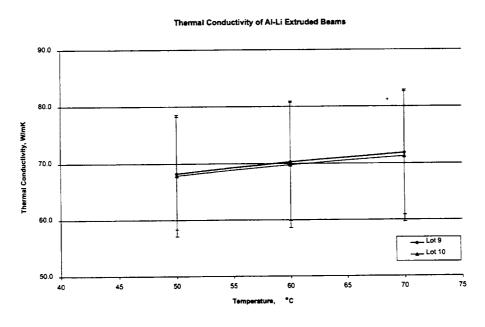


Figure 18. Thermal conductivity as a function of temperature for the Reynolds X2096-T8A3 Al-Li alloy extruded beams.

The specimens were nominally 10.2 cm in length and had a cross-section of 0.23 cm by 0.64 cm (see Appendix). The spacing between the thermocouples was nominally 4.5 cm and the frequency of the heat wave was 0.025 Hz. The measured values of thermal diffusivity from the six specimens did not vary much and were compiled together (see Figure 17). Thermal diffusivity measurements could only be made up to about $+70~^{\circ}\text{C}$. The density of this material was measured to be $2.57\pm0.01~\text{g/cm}^3$. A plot of the thermal conductivity is shown in Figure 18.

4.7.3 Coefficient of Thermal Expansion

Thermal expansion measurements were made on 12 51-mm long (2.0 inches) bars with rectangular cross-sections of ~ 6.4 x 2.3 mm (0.25 x 0.09 inches). The CTE measurements were made with a fused silica, push-rod dilatometer manufactured by The Edward Orton Jr. Ceramic Foundation. The Orton dilatometer uses an open-tube specimen holder and a push rod to transfer displacement outside of the thermal chamber to a linear variable-displacement transducer (LVDT). The specimen holder and push rod are made of fused silica. Thus the measured displacement is of the differential expansion of the material compared to that of fused silica (this is accounted for via instrument software). This test was conducted in accordance with ASTM E228-85 Standard Test Method for Linear Thermal Expansion of Solid Materials With a Vitreous Silica Dilatometer.

The operation of the instrument was validated with the measurement of a copper standard (NIST SRM 736) at the conclusion of the aluminum-lithium measurements.

The test specimens were heated from -171°C to 103°C at the rate of 3°C/min. The thermal expansion data was binned into 50° segments and fitted to a first-order polynomial. By definition, the derivative with respect to temperature of the thermal expansion curve is termed the "instantaneous" coefficient of thermal expansion. Hence the coefficient for the first-order term obtained from the linear fit is the measured CTE of the material. An average CTE at a given temperature was computed for the three specimens of one set of material, and the standard deviation incorporated into the estimated error of the measurement. A second component of the estimated error comes from the measurement of the copper standard and comparison with NIST CTE data. The average data for each set of specimens are provided in Table 11.

The results of thermal expansion measurements are shown in Figure 19. The CTE from these measurements is shown as a function of temperature in Figure 20. At first glance, there appears to be an apparent "drop" in CTE at +25°. Given that the drop is comparable in magnitude to the estimated uncertainty in that temperature range, it should **not** be presumed that the CTE does, in fact, decline with temperature near +25°C.

Table 11. Coefficient of Thermal Expansion vs. Temperature for X2096 Al-Li alloy

Temp	erature	Coefficient of Thermal Expansion (CTE), ppm/°C						AVG CTE		
°K	°c	AVG	STD	AVG	STD	AVG	STD	AVG	STD	Lot 9.
K		9L-1	DEV	9LT-I	DEV	10L-1	DEV	10LT-1	DEV	Lot 10,
		9L-1	DEV	9LT-2	DEV	10L-1	DEV	10LT-2	DEV	Lot 10, L and LT
		9L-2 9L-3		9LT-3		10L-2		10LT-2		LanuLi
140	105		0.0				2.0		0.0	00.5
148	-125	20.5	2.9	20.2	2.9	20.8	2.9	20.4	2.9	20.5
173	-100	20.7	1.7	20.5	1.6	21.1	1.6	20.9	1.6	20.8
248	-25	22.2	1.0	22.5	0.4	23.0	0.5	22.3	0.4	22.5
273	0	22.2	0.9	22.3	0.3	21.6	0.1	22.0	0.3	22.0
298	25	21.7	0.8	21.8	0.8	22.7	0.8	21.9	0.8	22.0
323	50	23.8	0.6	24.2	0.8	24.3	0.7	24.4	0.5	24.2
348	75	24.5	0.5	25.1	1.2	24.2	0.6	24.7	0.6	24.6

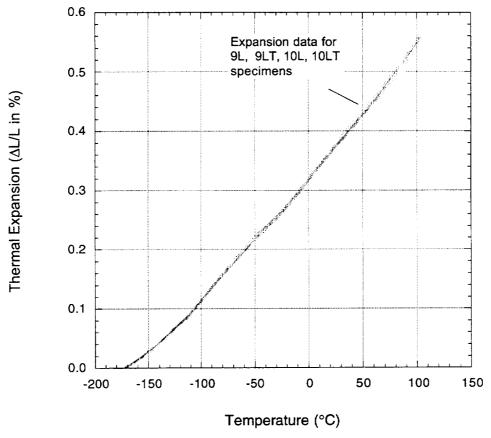


Figure 19. Linear expansion of the Reynolds X2096-T8A3 Al-Li alloy extruded beam specimens testing in L and LT directions.

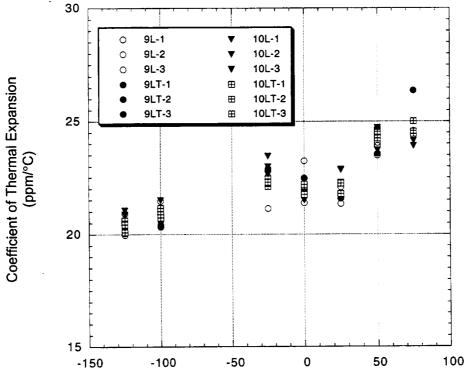


Figure 20. Coefficient of thermal expansion vs. temperature for the Reynolds X2096-T8A3 Al-Li alloy specimens.

4.8 Rivet Test

The Solar Array Support Structure is designed as a frame constructed of Al-Li extruded beams joined by rivets. A special test was conducted at GSFC in order to verify that riveting does not cause surface cracking in Al-Li X2096 alloy.

A total of four blanks were machined from the extruded beams. These blanks were assembled into two pairs and riveted together using NAS 1921-06 A-286 blind rivets. Exact geometry of the blank specimens is described in Appendix.

The riveted joints were cross sectioned and metallographically polished to examine the Al-Li surfaces which were in contact with the rivets. Figure 21 shows one of the cross sections taken along the rivet axis.

Inspection of all riveted specimens revealed no surface cracks in X2096-T8A3 Al-Li alloy, which indicates that riveting operation does not cause cracking in this alloy.

5.0 DISCUSSION

The X2096 alloy was offered for commercial use by the Reynolds Metals Company in mid-nineties (ref.5). Being one of the Weldalite 049 family of Al-Li alloys introduced by Martin Marietta around 1989 and early 1990, this alloy was developed to replace 7075-T6 for aircraft structural applications and featured a combination of low density, high strength and toughness (Ref. 6).

Despite the commercial availability of X2096, its mechanical properties are not readily available for the design purposes. Apparently, use of this alloy is still limited and, it has not been used in any production programs. Consequently, RMC did not produce sufficient quantity of this alloy to generate design database. Therefore, this alloy is yet to find its way into the industrial or government specifications and/or design data bases such as MILL HDBK 5, Aerospace Structural Metals Handbook, ASTM Standards or The Aluminum Standards and Data from the Aluminum Association, Inc., Aluminum Design Manual, etc.

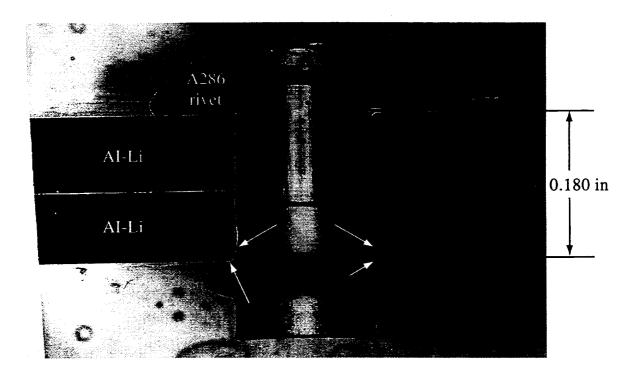


Figure 21 Longitudinal cross section of the riveted joint. White arrows point to the surfaces of the Al-Li alloy that were inspected for cracks.

Following the selection of X2096 alloy as a material of choice for HST SA3 structure, RMC produced two lots of the extruded beams. These beams were supposed to meet or exceed the requirements of the Goddard Specification LN-002297 (Ref 7).

This work was undertaken to verify that the Al-Li beams could meet the tensile and stress corrosion requirements and to evaluate shear, bearing, fracture, fatigue, and thermal properties of the X2096 alloy.

Due to small wall thickness of the extruded beams, all test loads were in-plane (normal to the product thickness). The total quantity of the extruded beams was marginal enough to support fabrication of the HST-SA3 structure. Consequently, the amount of beams available for machining of the test specimens was also very limited.

Since the HST-SA3 structure is fabricated from the mixed beams from both lots and an amount of beam material available for testing was limited, an assessment of the lot-to-lot variation of the mechanical properties of these beams was not practical within the scope of this effort. Nevertheless, the lot identity of each test specimen was maintained for the purpose of test record and in case a substantial difference in the measured properties between each lot was encountered, however unlikely.

In order to determine the minimum design values of the mechanical properties of the extruded beams, the direct computation procedure for the normal distribution (Ref. 8) was found to be most practical to handle statistical analysis of the results obtained in this work (see Table 12). However, due to the limited amount of material available for testing, the MIL-HDBK-5 requirements for sample size could not be met.

Table 12. Statistical Analysis of Results

PROPERTY	MEASURED VALUES	AVG	STD DEV	T ₉₉	T ₉₀
Ultimate Tensile Strength, TUS(L),ksi	82.66, 82.86, 76.00, 79.14, 79.5, 80.9, 80.2	80.18	2.34	69.32	72.74
* Ultimate Tensile Strength, TUS(LT),ksi	77.2, 76.5	76.85			
Tensile Yield Stress, TYS(L), ksi	78.3, 78.72, 71.06, 74.95, 71.5, 75.8, 74.9	75.03	2.98	61.22	65.97
* Tensile Yield Stress, TYS(LT), ksi	72.7, 70.4	71.55			
* Compression Yield Stress, CYS(L), ksi	79.4, 77.1	78.25			
* Compression Yield Stress, CYS(LT), ksi	78.8, 76.1	77.45			
Shear Ultimate Strength, SUS(L), ksi	47.68, 47.59, 47.65, 45.81, 47.52, 46.83, 46.70	47.11	0.70	43.86	44.70
Shear Ultimate Strength, SUS(LT), ksi	48.96, 48.1, 47.95, 47.07 47.66, 48.02	47.96	0.62	44.84	46.15
Bearing Ultimate Strength, BRU(L), ksi, e/d =2	149.9, 148.8, 150.4, 147.8, 144.3, 145, 149.6	147.97	2.43	136.71	140.21
Bearing Ultimate Strength, BRU(LT), ksi, e/d =2	150.3, 149.9, 150.6, 147.1 148.2, 147.5, 153.4	149.57	2.18	139.43	143.41
Bearing Ultimate Strength, BRU(L), ksi, e/d =1.5	115.5, 113.7, 115, 110.9, 107.8, 107.7, 111.6	111.74	3.19	96.92	101.98
Bearing Ultimate Strength, BRU(LT), ksi, e/d =1.5	114.3, 115.4, 113, 111, 112.8 115.3, 118.5	114.33	2.40	103.17	107.45
Modulus, E, ksi x 10 ³	10.96, 11.11, 10.88, 10.99 11.19, 11.25, 11.3, 11.29 11.15, 11.25, 11.26, 11.26 11.25, 11.22, 11.19, 11.34	11.18	0.13	10.74	10.93
	11.25				

Displayed in italic are the values received from RMC. Values of the properties marked by asterisk could not be statistically analyzed due to small sample size.

The following equations were used to derive lower tolerance bounds T values (Ref. 8):

$$T_{90} = \overline{X} - (k_{90} + 0.0338 - 0.202q_{LB}) \times S,$$
 and
$$T_{90} = \overline{X} - k_{90} \times S,$$

where T_{90} and T_{99} are lower tolerance bounds, \overline{X} is the average value of the properties measured, k_{90} and k_{99} are the one-sided tolerance—limit factors corresponding to T_{90} or T_{99} accordingly and S is the standard deviation. Other quantities present in the equation for T_{90} and the term q_{10} are empirical factors defined in Section 9.2.7, ref. 8, and are used to avoid "anticonservatism" in estimating lower tolerance bounds.

If these quantities were not used, the T_{90} bounds would be slightly higher. Table 9.6.4.1 in Ref. 8 was used to obtain k values.

The T_{90} indicates that at least 90% of the population of values of the beam properties is expected to equal or exceed the lower tolerance bound T_{90} with a confidence of 95%.

Likewise, the T_{99} means that at least 99% of the population of values is expected to equal or exceed the lower tolerance bound T_{99} with a confidence of 95%.

Lower tolerance bound T_{99} values for A-basis was estimated without anticonservative correction. Anticonservative correction was not necessary, since the limited sample size resulted in the T_{99} values already too low to be used as design allowables for HST-SA3.

Based on the risk analysis and design calculations, the project selected T_{on} values as design allowables for the HST SA3 structure.

6.0 CONCLUSIONS

In comparison to aluminum alloy 7075 in T6 and T73 tempers, the X2096-T8A3 Al-Li extruded beams displayed higher stiffness, shear and bearing strength values. Tensile properties of the tested beams did not appear to be superior to 7075-T6 extrusions, but much better than the ones for the T73 temper (Ref. 9). It should be realized, however, that an exact comparison is difficult to make, since no statistically significant values (such as A- or B-basis, for example, Ref. 8) were obtained in this work for X2096 alloy.

Crack growth rates for the X2096 extruded beams compared favorably with 7075-T6,T73. Al-Li alloy had a higher threshold stress concentration value than 7075. This means that X2096 material is more resistant to crack initiation. Fatigue life of X2096 in fully reversed bending shows endurance limit around 15 ksi. The fatigue behavior of 7075-T6 (Ref. 10) is very similar to X2096 in the range between 500,000 and 30,000 cycles.

The X2096 extruded beams display very good resistance to stress-corrosion cracking as evidenced by no failures during the 30-day alternative immersion stress-corrosion test performed by RMC. This is a significant factor if compared with 7075-T6, known for its low resistance to stress corrosion cracking (Ref. 11).

In-plane anisotropy observed in the X2096-T8A3 extrusions in the course of this work was very moderate and no worse than that of 7075 extrusions.

Overall, considerable weight savings due to lower density (2.63 g/cm³ as compared to 2.8 g/cm³ for 7075) and good in-plane mechanical properties of the RMC X2096 Al-Li alloy made it very attractive material for the HST SA3 application.

A word of caution, however, should be said about the out-of-plane properties of the X2096 extrusions. Although direct measurements of the mechanical properties in short transverse direction could not be performed due to small wall thickness of the extruded beams, a clear indication of the heavily laminated structure of the beams was evidenced in this work during the test specimen preparation (see Figures 22 and 23). It is not recommended, therefore, to use this material in applications where short-transverse properties are critical.

Finally, it is important to understand that this test program measured the properties specific only to the two isolated ingots of X2096 Al-Li alloy, from which Lot 9 and Lot 10 extrusions were made. The results of this work can not be used as a general design property reference for the X2096-T6A3 extrusions. Instead, the data obtained can serve as a bench mark specific to an isolated quantity of this material. Furthermore, the data should be treated as representing a single production run by RMC. The properties of the future production runs must be verified via either lot release tests provided by the manufacture or an independent tests by the customer or any combination of them.

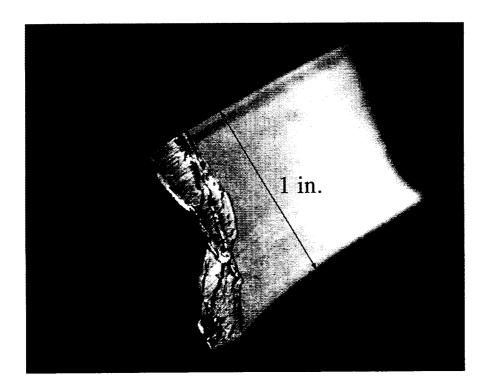


Figure 22. Fracture surface of the broken strip machined from the X2096-T8A3 extrusion. Note severe delamination.

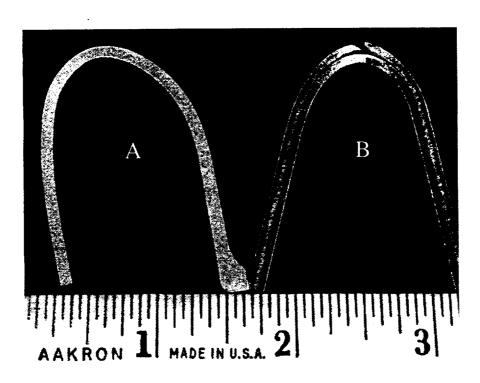


Figure 23. Behavior of the X2096-T8A3 strip machined from the extruded beam in transverse (a) and longitudinal (b) bending. Note delamination in longitudinal bend.

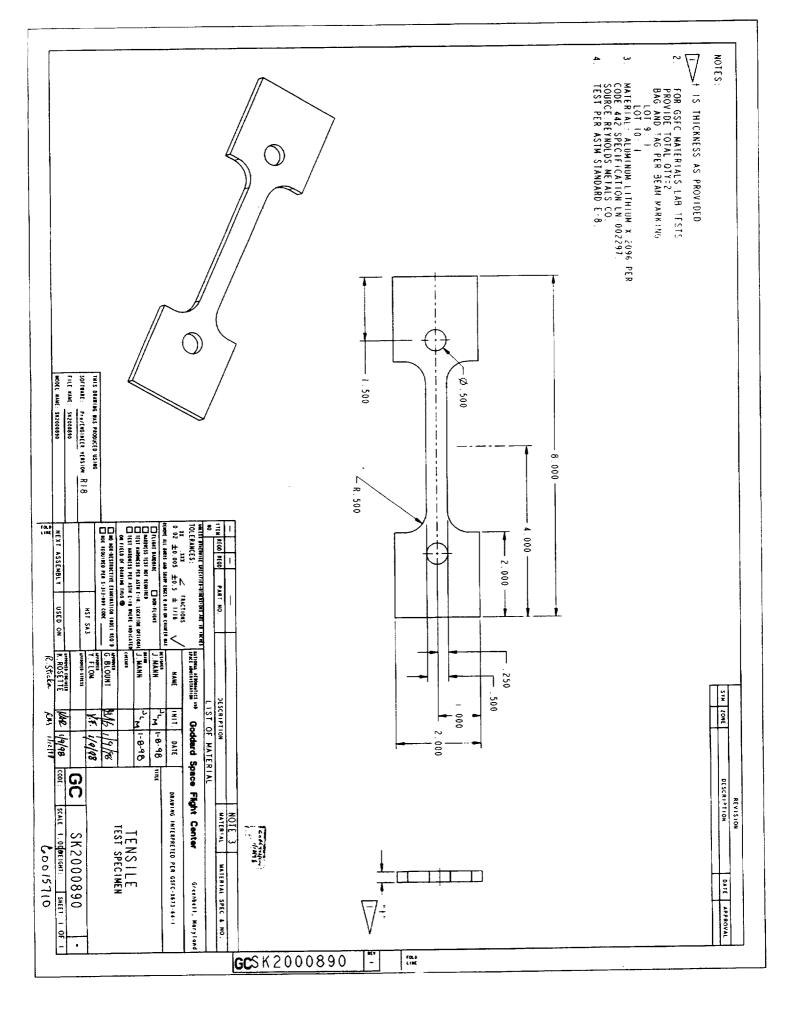
List of References

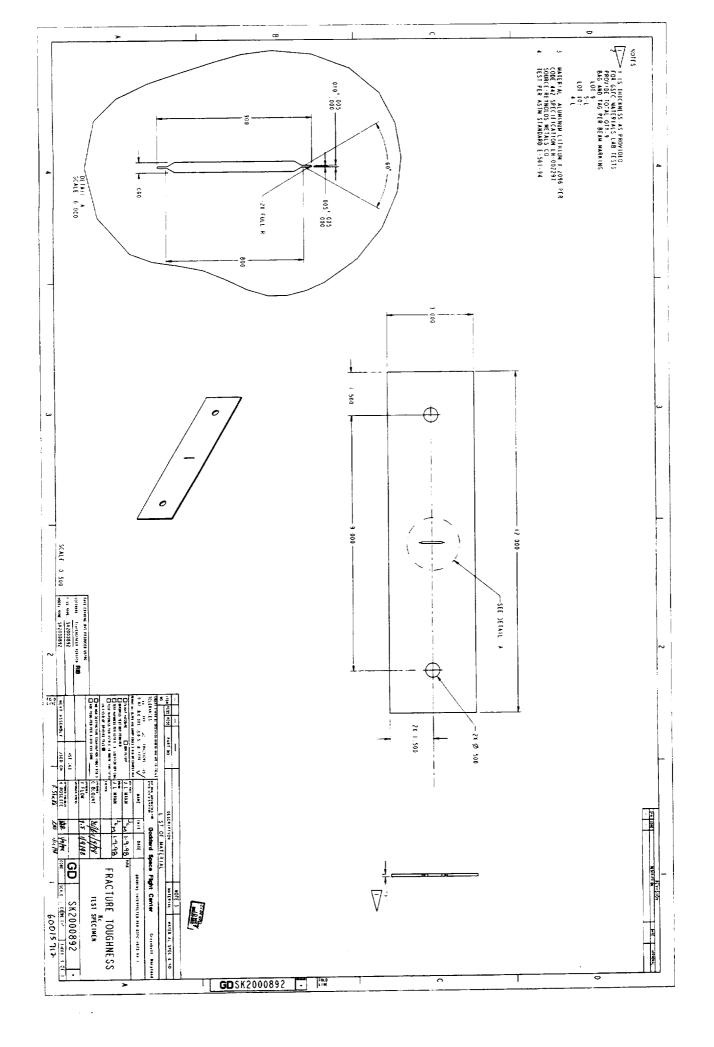
- 1. Alex Cho, "Properties of Reynolds Al-Li alloy X2096-T8A3 Extruded Beams For HST Solar Array Support," Letter submitted to GSFC on April 15, 1998.
- 2. J. G. Kaufman and R. E. Davis, "Effects of Test Method and Specimen Orientation on Shear Strengths of Aluminum Alloys," Proc., Vol. 64, 67th Ann. Mtg. ASTM, Chicago, June 21-26, 1964
- 3. NASA TM 104629, "Determination of Elastic Moduli of Fiber Resin Composites Using an Impulse Excitation Technique," Viens and Johnson, February 1996.
- 4. Y.S. Touloukian, R.W. Powell, C.Y. Ho, and Nicolaou, M.C., Thermal Diffusivity, Vol. 10 of Thermophysical Properties of Mattter, The TPRC Data Series, pp. 28a-37a, IFI/Plenum Data Corp., N.Y. 1973.
- 5. R.J. Rioja, R. H. Graham, Advanced Materials and Processes, June 1992, pp.23-26.
- 6. B.N. Bhat, T.T. Bales, and E.J. Vesely, Jr., NASA Conference Publication 3287, December 1994, pp.11-26
- 7. Material Specification for Aluminum Alloy X2096-T8A3 for the Hubble Space Telescope Rigid Solar Array, LN-002297, SAI-SPEC-0396, Goddard Space Flight Center, September 1997.
- 8. Metallic Materials and Elements for Aerospace Vehicle Structures, MIL-HDBK-5G, 1 November 1994.
- 9. "NASA/FLAGRO" computer program, v. 2.0, revision A, May 1994
- 10. Aerospace Structural Metals Handbook, U.S. Air Force, NASA, published by CINDAS/Purdue University.
- 11. Design Criteria for Controlling Stress Corrosion Cracking, MSFC-SPEC-522B, July 1, 1987

•	

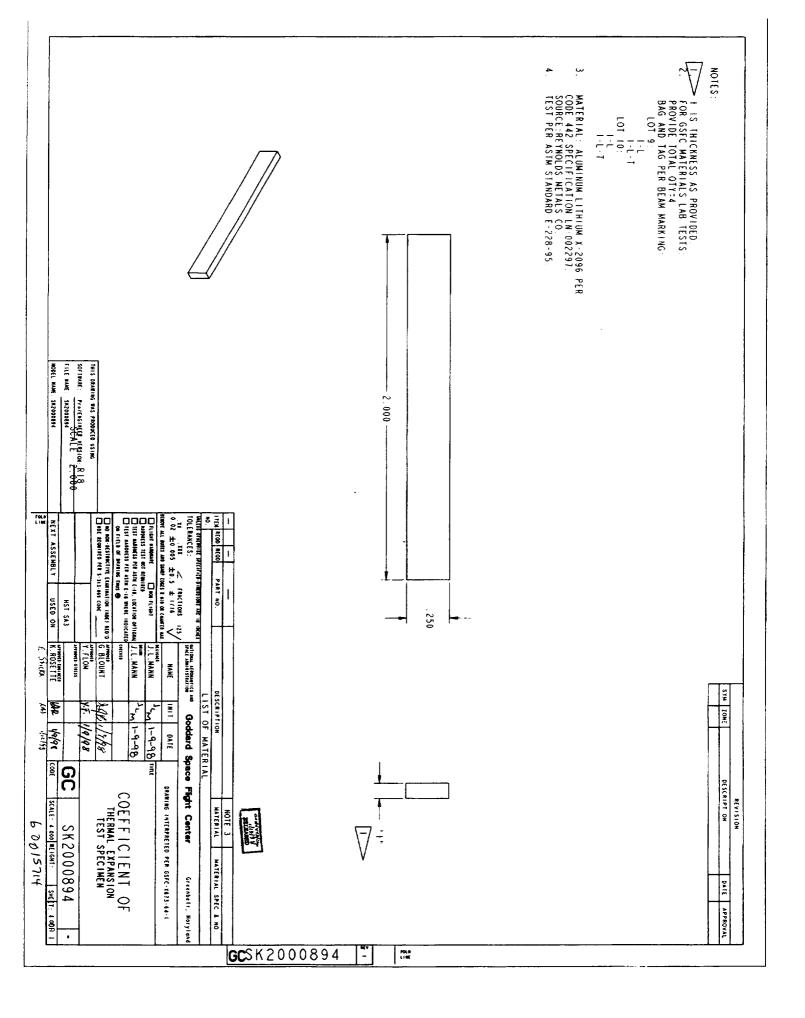
Attachment

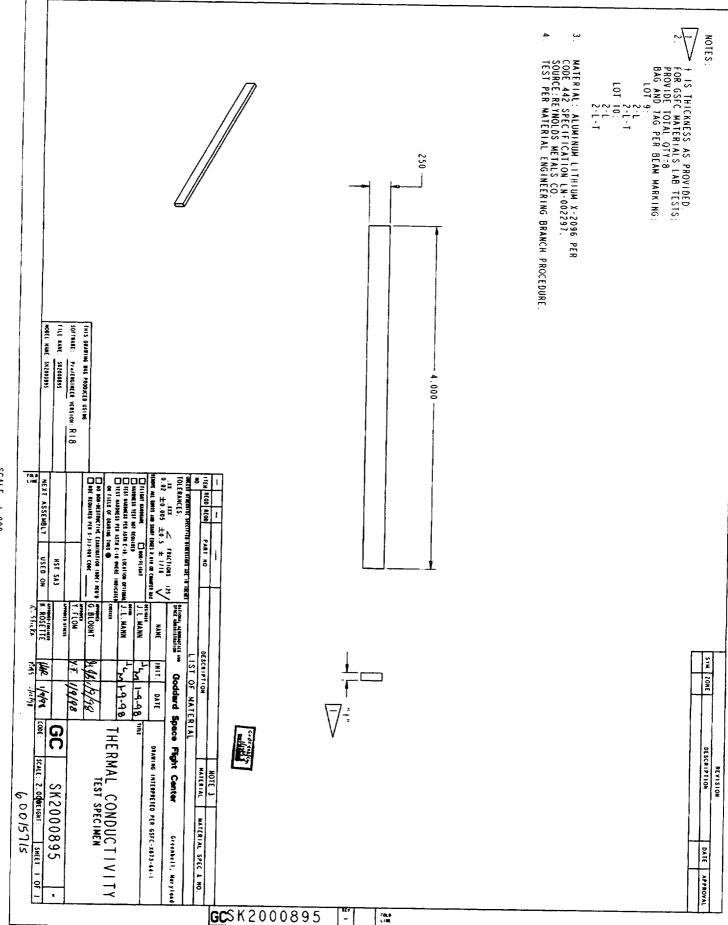
,		
t .		
		•





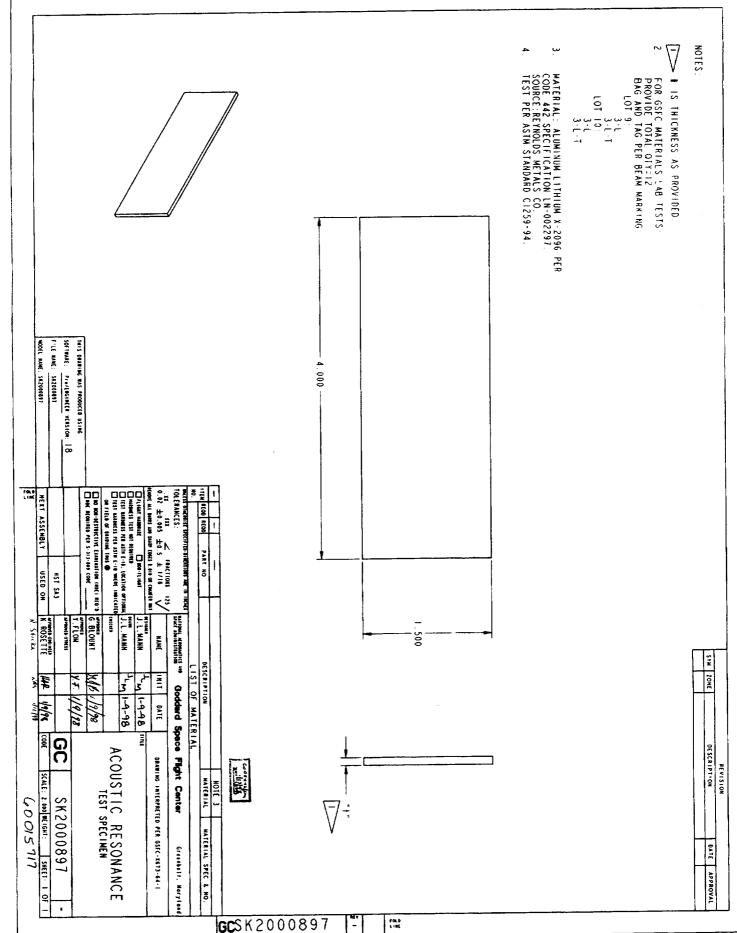
SCALE 1.000





SCALE 1,000

SCALE 1.000



SCALE 1.000

SCALE 1.000

CALE | .000

REPORT DOCUMENTATION PAGE

Form Approved OMB No. 0704-0188

1. AGENCY USE ONLY (Leave blank)	2. REPORT DATE August 1999	3. REPORT TYPE AN Technical	ID DATES COVERED Publication
4. TITLE AND SUBTITLE			5. FUNDING NUMBERS
Evaluation Of Engineering P	roperties		
Of Al-Li Alloy X2096-T8A3	Extrusion Products		
5. AUTHOR(S)	·-·		ł
s. Admon(s)			
Y. Flom, M. Viens, L. Wang			
7. PERFORMING ORGANIZATION NAM	E(S) AND ADDRESS (ES)		8. PEFORMING ORGANIZATION
Materials Engineering Branch	n		REPORT NUMBER
Goddard Space Flight Center			
Greenbelt, Maryland 20771			
			99B00033
9. SPONSORING / MONITORING AGEN	CY NAME(S) AND ADDRESS	S (ES)	10. SPONSORING / MONITORING
			AGENCY REPORT NUMBER
National Aeronautics and Space	Administration		
Washington, DC 20546-0001			TP1999-209203
		į	
1. SUPPLEMENTARY NOTES			
L. Wang			
L. Wang UNISYS - 7600 Boston Way,	Lanham, Maryland 2	0706	
UNISYS - 7600 Boston Way,	•	0706	12b. DISTRIBUTION CODE
UNISYS - 7600 Boston Way, 2a. DISTRIBUTION / AVAILABILITY STA Unclassified - Unlimited	•	0706	12b. DISTRIBUTION CODE
UNISYS - 7600 Boston Way, 2a. DISTRIBUTION / AVAILABILITY STA	•	0706	12b. DISTRIBUTION CODE
UNISYS - 7600 Boston Way, 2a. DISTRIBUTION / AVAILABILITY STA Unclassified - Unlimited Subject Category: 39 Report available from the NASA	TEMENT A Center for AeroSpace	Information,	12b. DISTRIBUTION CODE
UNISYS - 7600 Boston Way, 2a. DISTRIBUTION / AVAILABILITY STA Unclassified - Unlimited Subject Category: 39	TEMENT A Center for AeroSpace	Information,	12b. DISTRIBUTION CODE
UNISYS - 7600 Boston Way, 2a. DISTRIBUTION / AVAILABILITY STA Unclassified - Unlimited Subject Category: 39 Report available from the NASA Parkway Center/7121 Standard	TEMENT A Center for AeroSpace	Information,	12b. DISTRIBUTION CODE
UNISYS - 7600 Boston Way, 2a. DISTRIBUTION / AVAILABILITY STA Unclassified - Unlimited Subject Category: 39 Report available from the NASA Parkway Center/7121 Standard 3. ABSTRACT (Maximum 200 words)	A Center for AeroSpace Drive, Hanover, Maryla	Information, nd 21076-1320	
UNISYS - 7600 Boston Way, 2a. DISTRIBUTION / AVAILABILITY STA Unclassified - Unlimited Subject Category: 39 Report available from the NASA Parkway Center/7121 Standard 3. ABSTRACT (Maximum 200 words) Mechanical, thermal, fatigue	A Center for AeroSpace Drive, Hanover, Maryla and stress corrosion p	Information, and 21076-1320 roperties were determined to the control of the contr	nined for the two lots of Al-
UNISYS - 7600 Boston Way, 2a. DISTRIBUTION / AVAILABILITY STA Unclassified - Unlimited Subject Category: 39 Report available from the NASA Parkway Center/7121 Standard 3. ABSTRACT (Maximum 200 words)	A Center for AeroSpace Drive, Hanover, Maryla and stress corrosion p	Information, and 21076-1320 roperties were determined to the control of the contr	nined for the two lots of Al-
UNISYS - 7600 Boston Way, 2a. DISTRIBUTION / AVAILABILITY STA Unclassified - Unlimited Subject Category: 39 Report available from the NASA Parkway Center/7121 Standard 3. ABSTRACT (Maximum 200 words) Mechanical, thermal, fatigue a	A Center for AeroSpace Drive, Hanover, Maryla and stress corrosion poms. Based on the test	Information, and 21076-1320 roperties were determant results, the beams we	nined for the two lots of Alere accepted as the construc-
UNISYS - 7600 Boston Way, 2a. DISTRIBUTION / AVAILABILITY STA Unclassified - Unlimited Subject Category: 39 Report available from the NASA Parkway Center/7121 Standard 3. ABSTRACT (Maximum 200 words) Mechanical, thermal, fatigue a Li X2096-T8A3 extruded bea	A Center for AeroSpace Drive, Hanover, Maryla and stress corrosion poms. Based on the test	Information, and 21076-1320 roperties were determant results, the beams we	nined for the two lots of Alere accepted as the construc-
UNISYS - 7600 Boston Way, 2a. DISTRIBUTION / AVAILABILITY STA Unclassified - Unlimited Subject Category: 39 Report available from the NASA Parkway Center/7121 Standard 3. ABSTRACT (Maximum 200 words) Mechanical, thermal, fatigue a Li X2096-T8A3 extruded bea	A Center for AeroSpace Drive, Hanover, Maryla and stress corrosion poms. Based on the test	Information, and 21076-1320 roperties were determant results, the beams we	nined for the two lots of Alere accepted as the construc-
UNISYS - 7600 Boston Way, Pa. DISTRIBUTION / AVAILABILITY STA Unclassified - Unlimited Subject Category: 39 Report available from the NASA Parkway Center/7121 Standard B. ABSTRACT (Maximum 200 words) Mechanical, thermal, fatigue a Li X2096-T8A3 extruded bea	A Center for AeroSpace Drive, Hanover, Maryla and stress corrosion poms. Based on the test	Information, and 21076-1320 roperties were determant results, the beams we	nined for the two lots of Alere accepted as the construc-
UNISYS - 7600 Boston Way, 2a. DISTRIBUTION / AVAILABILITY STA Unclassified - Unlimited Subject Category: 39 Report available from the NASA Parkway Center/7121 Standard 3. ABSTRACT (Maximum 200 words) Mechanical, thermal, fatigue a Li X2096-T8A3 extruded bea	A Center for AeroSpace Drive, Hanover, Maryla and stress corrosion poms. Based on the test	Information, and 21076-1320 roperties were determant results, the beams we	nined for the two lots of Alere accepted as the construc-
UNISYS - 7600 Boston Way, 2a. DISTRIBUTION / AVAILABILITY STA Unclassified - Unlimited Subject Category: 39 Report available from the NASA Parkway Center/7121 Standard 3. ABSTRACT (Maximum 200 words) Mechanical, thermal, fatigue a Li X2096-T8A3 extruded bea	A Center for AeroSpace Drive, Hanover, Maryla and stress corrosion poms. Based on the test	Information, and 21076-1320 roperties were determant results, the beams we	nined for the two lots of Alere accepted as the construc-
UNISYS - 7600 Boston Way, 2a. DISTRIBUTION / AVAILABILITY STA Unclassified - Unlimited Subject Category: 39 Report available from the NASA Parkway Center/7121 Standard 3. ABSTRACT (Maximum 200 words) Mechanical, thermal, fatigue a Li X2096-T8A3 extruded bea	A Center for AeroSpace Drive, Hanover, Maryla and stress corrosion poms. Based on the test	Information, and 21076-1320 roperties were determant results, the beams we	nined for the two lots of Alere accepted as the construc-
UNISYS - 7600 Boston Way, 2a. DISTRIBUTION / AVAILABILITY STA Unclassified - Unlimited Subject Category: 39 Report available from the NASA Parkway Center/7121 Standard 3. ABSTRACT (Maximum 200 words) Mechanical, thermal, fatigue a Li X2096-T8A3 extruded bea	A Center for AeroSpace Drive, Hanover, Maryla and stress corrosion poms. Based on the test	Information, and 21076-1320 roperties were determant results, the beams we	nined for the two lots of Alere accepted as the construc-
UNISYS - 7600 Boston Way, Pa. DISTRIBUTION / AVAILABILITY STA Unclassified - Unlimited Subject Category: 39 Report available from the NASA Parkway Center/7121 Standard B. ABSTRACT (Maximum 200 words) Mechanical, thermal, fatigue a Li X2096-T8A3 extruded bea	A Center for AeroSpace Drive, Hanover, Maryla and stress corrosion poms. Based on the test	Information, and 21076-1320 roperties were determant results, the beams we	nined for the two lots of Alere accepted as the construc-

14. SUBJECT TERMS

Engineering, Properties, Al-Li Alloys

15. NUMBER OF PAGES

16. PRICE CODE

17. SECURITY CLASSIFICATION OF REPORT 18. SECURITY CLASSIFICATION OF THIS PAGE Unclassified

Unclassified

19. SECURITY CLASSIFICATION OF ABSTRACT Unclassified

20. LIMITATION OF ABSTRACT

UL